THE JOURNAL OF BIOLOGICAL CHEMISTRY VOL. 286, NO. 30, pp. 26431–26439, July 29, 2011

Stimulation of Yeast Telomerase Activity by the Ever Shorter Telomere 3 (Est3) Subunit Is Dependent on Direct Interaction with the Catalytic Protein Est2*[S]

Received for publication, February 7, 2011, and in revised form, June 8, 2011 Published, JBC Papers in Press, June 9, 2011, DOI 10.1074/jbc.M111.228635

Jennell M. Talley[‡1], Diane C. DeZwaan[§2], Leslie D. Maness[‡], Brian C. Freeman[§], and Katherine L. Friedman[‡3]

From the [‡]Department of Biological Sciences, Vanderbilt University, Nashville, Tennessee 37235 and the [§]Department of Cell and Developmental Biology, University of Illinois at Urbana-Champaign, Urbana, Illinois 61801

Telomerase is a multisubunit enzyme that maintains genome stability through its role in telomere replication. Although the Est3 protein is long recognized as an essential telomerase component, how it associates with and functions in the telomerase complex has remained enigmatic. Here we provide the first evidence of a direct interaction between *Saccharomyces cerevisiae* Est3p and the catalytic protein subunit (Est2p) by demonstrating that recombinant Est3p binds the purified telomerase essential N-terminal (TEN) domain of Est2p *in vitro*. Mutations in a small cluster of amino acids predicted to lie on the surface of Est3p disrupt this interaction with Est2p, reduce assembly of Est3p with telomerase *in vivo*, and cause telomere shortening and senescence. We also show that recombinant Est3p stimulates telomerase activity above basal levels *in vitro* in a manner dependent on the Est2p TEN domain interaction. Together, these results define a direct binding interaction between Est3p and Est2p and reconcile the effect of *S. cerevisiae* Est3p with previous experiments showing that Est3p homologs in related yeast species influence telomerase activity. Additionally, it contributes functional support to the idea that Est3p is structurally related to the mammalian shelterin protein, TPP1, which also influences telomerase activity through interaction with the Est2p homolog, TERT.

Telomeres are protein-DNA complexes that protect chromosome termini from nucleolytic digestion and distinguish natural chromosome ends from internal DNA breaks. Although the majority of telomeric DNA is double stranded, the G/T-rich strand forms a protruding 3′-overhang. In the absence of a counteracting mechanism, telomeres shorten during each cell division, ultimately activating cell cycle checkpoints and cellular senescence (1). If these checkpoints are disrupted or bypassed, end-to-end fusions and bridge breakage cycles can ensue. Telomerase, a ribonucleoprotein complex, promotes telomere maintenance and genomic stability by elongating the 3′-overhang by reverse transcription (2).

In budding yeast, telomerase consists minimally of four dedicated subunits: TLC1 RNA, the template RNA (3); Est1p, an accessory protein important for recruiting and activating telomerase at the telomere (4, 5); Est2p, the reverse transcriptase (2); and Est3p, an additional accessory protein necessary for proper activity *in vivo* (6). Deletion of any of these components eliminates telomerase function *in vivo*, yielding the **E**ver **S**horter **T**elomere (EST)[4] phenotype (3, 7, 8).

Although these and other telomerase components have been known for well over a decade, few details of their assembly into the ribonucleoprotein complex are understood. Described interactions are largely confined to protein associations with the RNA template. Est1p and Est2p independently bind distinct regions within the central portion of TLC1 RNA (9–11). Sm proteins facilitate RNA stability through interaction with a site near the 3′-end of the RNA (12), and association of the catalytic core of telomerase with the telomere in G_1 phase is mediated by interaction of the yKu heterodimer with TLC1 RNA (13). Protein/protein interactions are less well understood. Est1p and Est2p may interact in an RNA-independent manner (5, 14). When Est1p is tethered to an internal chromosomal site via fusion with the Gal4 DNA binding domain, Est2p is recruited to that site in the absence of TLC1 RNA (14). Furthermore, recombinant Est1p and Est2p can bind directly, although TLC1 RNA enhances this interaction (5).

Both the function of Est3p and the mechanism of its assembly into the telomerase complex are unknown. Est1p stimulates the association of Est3p with telomerase in a cell cycle-dependent manner that requires Est2p (15). Very recently, Est1 protein purified from yeast was shown to bind recombinant Est3 protein, yielding strong evidence for a direct interaction between these two proteins (16). Genetic evidence suggests that Est3p interacts with the N-terminal (TEN) domain of Est2p, but no direct protein/protein or protein/RNA interactions have been reported (6, 17, 18). It has been suggested that Est3p binds nucleic acid and possesses helicase activity (19). However, sensitive analysis by NMR spectroscopy of Est3p in the presence and absence of DNA failed to detect an interaction (18).

Although Est3p has been reported to be dispensable for the catalytic activity of *Saccharomyces cerevisiae* telomerase (20),

* This work was supported, in whole or in part, by National Institutes of Health Grant GM080393. This work was also supported by Vanderbilt Discovery Grant (to K. L. F.).

[S] The on-line version of this article (available at http://www.jbc.org) contains supplemental Figs. S1–S3 and Tables S1 and S2.

[1] Supported in part by National Institutes of Health Grant T32 GM08554.

[2] Supported by a Computational Molecular Biology-National Institutes of Health training grant. Present address: Dept. of Anatomy and Cell Biology, the University of Iowa, Iowa City, IA 52242.

[3] To whom correspondence should be addressed: Vanderbilt University Station B, Box 351634, Nashville, TN 37235. Fax: 615-343-6707; E-mail: katherine.friedman@vanderbilt.edu.

[4] The abbreviations used are: EST, ever shorter telomere; MBP, maltose-binding protein; OB, oligonucleotide/oligosaccharide-binding; TEN, telomerase essential N-terminal.

recent work in the related species *Saccharomyces castelli* implicates the Est3p homolog in stimulating nucleotide addition processivity (18). In addition, Est3p from *Candida albicans* is required for robust telomerase activity *in vitro* with specific primers (21). These data raise the possibility that Est3p affects enzymatic activity in *S. cerevisiae* but that technical limitations have, to date, precluded the detection of such effects.

Here we show the first biochemical evidence that Est3p binds directly to the TEN domain of Est2p. We also show that recombinant Est3p stimulates telomerase activity during *in vitro* primer extension and that the interaction of Est3p with the Est2p TEN domain appears required for this function.

EXPERIMENTAL PROCEDURES

Plasmid and Strain Construction

Plasmids for Protein Expression—The plasmid pET Duet EST3 (for expression of *His_6-EST3*) was made by moving *EST3* from YCPlac33 EST3 using primers M090 and M091 (supplemental Table S1) into pET Duet-1 (Novagen) using restriction sites BamHI and SalI. *EST3* mutants *K71A* (lysine 71 to alanine), *ETN* (glutamate 114, threonine 115, and asparagine 117), and *DQ* (aspartate 166 and glutamine 167) were introduced into pET Duet EST3 by QuikChange™ (Stratagene) using primer pairs K71A forward and K71A reverse, ETN114AAK forward and ETN114AAK reverse, and DQ forward and DQ reverse, respectively. A vector for expression of *MBP-EST2^{TEN}* was made by cloning *EST2 ^{TEN}* (residues 1–162) from pKF404 (22) using primer pair LM204.1 forward and LM204.1 reverse into pLM204a (gift of L. Mizoue) using restriction sites EcoRI and PstI. The *MBP-EST2^{TEN}* fusion gene was then moved into the EcoRV and KpnI sites of pET Duet-1 using primer pair EcoRV MBP forward and KpnI Est2RI reverse to create pET Duet MBP-EST2^{TEN}. *MBP* alone was cloned into the EcoRV and KpnI restriction sites of pET Duet-1 from pLM204a using primer pair EcoRV MBP forward and KpnI MBP reverse to create pET Duet MBP.

Plasmids for in Vivo Characterization—pKF441 (*CEN EST3 URA3*) was created by PCR amplification of the *EST3* promoter and frameshift-corrected gene from pVL901 (gift of V. Lundblad) using primer pair UEprimer1 and UEprimer4 to create an EcoRI site upstream of the promoter and a KpnI site immediately before the *EST3* stop codon. The endogenous *EST3* termination sequence was amplified using primer pairs UEprimer5 and UEprimer6 to create a HindIII site downstream of the terminator. UEprimer1 and UEprimer6 were then used to amplify the full-length insert using these two PCR products as templates. The resulting fragment was cloned into YCplac33 (*CEN URA3*) using EcoRI and HindIII. pKF442 (*CEN EST3HA URA3*) was created by PCR amplification of the HA_3 tag from pVL901 using primer pair KpnI forward and XbaI reverse and ligation into pKF441 using KpnI and XbaI. *EST3* and *EST3HA* were subsequently moved into pRS315 or pRS425 (*CEN LEU2* and 2 μm *LEU2*, respectively) (23, 24) using the PvuII sites of pKF441 or pKF442. The *ETN* and *K71A* alleles were subcloned from pET Duet-1 (see above) using restriction sites MscI and XhoI. *DQ* was created by QuikChange™ using the same primers as above and subcloned using SpeI and XmaI. All point mutations were verified by sequencing.

Yeast Strains

YKF122 (AVL78 *est3::KAN^R*) was created by standard one-step gene replacement. The kanamycin-resistance gene was amplified by PCR from pFA6a-kanMX6 using primers Est3Kan forward and Est3Kan reverse. The PCR product was cloned into the SacI and KpnI sites of pKF441 to create pKF441 *est3::KAN*. The deletion construct was transformed into AVL78 using a standard lithium acetate protocol. YKF126 (AVL78 *est3::KAN^R EST2-G_8-Myc_{18}* (G: glycine)) was created by linearizing pRS304-Est2-G8-Myc18 (gift of V. Zakian) with SwaI and transforming it into YKF122 + pKF441. Strains and plasmids used in this study are shown in supplemental Table S2.

Complementation and Growth Assay

Functional complementation of the *est3* mutant alleles was tested in YKF122 (AVL78 *est3::KAN^R*) using mutant constructs created in pRS315 (*CEN LEU2*). YKF122 was complemented with pKF442 (*CEN EST3HA URA3*); loss of the complementing plasmid was selected on 5-fluoroorotic acid plates, and the wild-type or mutant pRS315 plasmids were subsequently transformed using the standard lithium acetate method. Resulting single colonies were restreaked three times on plates lacking leucine. Cell viability was assessed visually, and telomere length was determined by Southern blotting using XhoI as described previously (17).

Protein Purification

BL21 cells containing pET Duet *EST3* were grown in 6 liters of standard Luria broth (LB) with 50 μg/ml ampicillin at 37 °C to an A_{600} 0.3–0.4. After shifting the culture to 16 °C for 1 h, protein expression was induced with 500 μM isopropyl 1-thio-β-D-galactopyranoside overnight with moderate shaking (110 rpm). Cells were harvested by centrifugation at 4 °C and resuspended in 10 ml of TG buffer (+100 mM NaCl) per liter of original culture (TG: 50 mM Tris, pH 7.5, 10% glycerol, and 3 mM β-mercaptoethanol). Cells were lysed using an EmulsiFlex (Avestin) by passing cells three or four times through the machine at 20,000 psi. The resulting extract (60 ml) was incubated with 7.5 ml of Talon® resin (Clontech) for 1 h at 4 °C with gentle agitation and gravity-packed into an empty glass Econo-Column™ (Bio-Rad). Resin was washed with 10 column volumes of TG + 300 mM NaCl and 10 mM imidazole. Protein was eluted with 5 column volumes TG + 100 mM NaCl and 100 mM imidazole. The eluate was dialyzed (Spectra/Por® no. 7; 10,000-kDa (Spectrum Laboratories)) at 4 °C overnight into TG buffer, bound to a Source™ 15Q HR16/10 column (GE Healthcare), and eluted using a linear salt gradient (TG + 0 mM NaCl to TG + 1 M NaCl). The purest fractions were pooled and applied to a Superdex™ 200 26/60 gel filtration column (GE Healthcare) using TG + 100 mM NaCl buffer. Again, His_6-Est3p fractions were pooled and concentrated to 3 ml using a 15-ml, 10-kDa cutoff Amicon® ultraconcentrator (Millipore) and dialyzed into TG + 100 mM NaCl + 50% glycerol. The protein was stored at −20 °C. Mutant proteins were purified in the same

manner except that *ETN* and *DQ* were purified at pH 8.0. The Est3 protein sequence was verified by mass spectrometry.

Three-liter cultures of BL21 cells containing pET Duet *MBP-EST2^{TEN}* were grown and harvested as described above. Cells were lysed as above in 10 ml of TEG-200 per liter of original culture (TEG-200: 20 mM Tris-HCl, pH 7.4, 200 mM NaCl, 1 mM EDTA, 10% glycerol). Extract was incubated with 10 ml of amylose resin for 2 h at 4 °C and was packed similarly as above. Resin was washed with 15 column volumes of TEG + 500 mM NaCl. MBP-Est2p^{TEN} was eluted with TEG-200 + 5 mM maltose. Fractions containing MBP-Est2p^{TEN} were further purified over an S200 gel filtration column using TG + 100 mM NaCl buffer. MBP-Est2p^{TEN} was concentrated as described for His$_6$-Est3p and dialyzed into TG + 100 mM NaCl, 50% glycerol. Protein was stored at −20 °C. The Est2^{TEN} protein sequence was verified by mass spectrometry.

All purified proteins were separated by 12% SDS-PAGE to determine purity. All protein preparations used were judged by Bio-Safe^{TM} Coomassie (Bio-Rad) staining to be at least 95% pure. Protein concentration was determined either by spectrophotometry or by comparison of a serial dilution with a known concentration of protein standard. Maltose-binding protein (MBP) was purchased from New England Biolabs and diluted to 20 μM in TG + 100 mM NaCl + 50% glycerol.

In Vitro Pulldown Assay, Immunoprecipitation, and Western Blot Analysis

MBP or MBP-Est2p^{TEN} (200 pmol) was incubated with 25 μl of amylose resin in buffer I (20 mM Tris-HCl, pH 7.4, 200 mM NaCl, 1 mM EDTA, 0.05% Tween 20, and 10% glycerol) for 2 h at 4 °C with gentle agitation. 1 nmol of His$_6$-Est3p or mutant Est3 protein was added and incubated for 3 h at 4 °C. The resin was washed three times for 5 min with 1 ml of buffer I, resuspended in 100 μl of buffer I, loaded into a 700-μl spin cup (Pierce), and washed with 1.5 ml of buffer I. Retained resin was resuspended in 40 μl of buffer I, and 20 μl was separated by 12% SDS-PAGE. For detection of MBP and MBP-Est2p^{TEN}, proteins were blotted onto nitrocellulose (GE Healthcare) and blocked with 5% milk/PBS, pH 7.4, with 0.05% Tween (PBS-T). For detection of His$_6$-Est3, proteins were blotted onto Hybond P membrane (GE Healthcare) and blocked with 5% BSA/PBS-T. HRP-conjugated anti-MBP (New England Biolabs) was used at a dilution of 1:50,000 in 5% milk/PBS-T. Primary antibody for detection of the His$_6$ tag (Santa Cruz Biotechnology) was diluted 1:1,000 in 5% BSA/PBS-T. Secondary antibody was peroxidase-conjugated mouse anti-rabbit (Chemicon) at 1:10,000 in 5% milk/PBS-T. ECL plus Western Blotting Detection system (GE Healthcare) was used for detection.

Yeast protein extract was prepared as described (22). Extracts were normalized to 20 mg/ml and incubated with antibodies as described previously (15, 22). 10 μl of anti-Myc immunoprecipitated material (1/6 of total) or anti-HA immunoprecipitated material was separated by 10–12% step-gradient SDS-PAGE. Proteins were transferred to Hybond P membrane (GE Healthcare). The membrane was blocked with 5% milk/PBS-T followed by incubation with primary antibodies (HA: 1:500 dilution murine monoclonal HA.11 (Covance) or Myc: 1:250 dilution of murine monoclonal Myc Ab-1 (OP10L, EMD Biosciences)) in 5% milk/PBS-T. Secondary antibody was peroxidase-conjugated goat anti-mouse (Chemicon) used at a 1:10,000 dilution in 5% milk/PBS-T. Detection was done as described above.

Telomerase Assay and Northern Blot Analysis

Telomerase was partially purified from wild-type yeast (YPH499) by chromatography over DEAE-Sepharose fast flow resin (GE Healthcare) and Mono Q resin (GE Healthcare) as described previously (5, 25) and used in telomerase DNA extension assays. Briefly, partially purified telomerase extract was incubated with 2 pmol of a 7-base 3′-overhang template (GTGTGTG) immobilized on streptavidin paramagnetic beads (Promega) and extension buffer (50 mM Tris, pH 8.0, 1 mM $MgCl_2$, 1 mM spermidine, 1 mM DTT, 0.5% glycerol, 50 μM dTTP, 10 μCi of [α-^{32}P]dGTP (3,000 Ci mmol^{-1}; Amersham Biosciences)). The 7-base 3′-overhang template was generated by annealing biotin-conjugated Backbone1 primer (supplemental Table S1) to GTG7 base consensus primer. Reactions were incubated for 30 min at 30 °C followed by magnetic collection of DNA-bound beads. The beads were washed twice with 1 × EcoRI buffer (New England Biolabs). Beads were resuspended in 50 μl of 1 × EcoRI buffer, 100 μg/ml BSA, and 10 units of EcoRI and incubated for 1 h at 37 °C. The beads and cleaved DNA fragments were separated magnetically. A PNK (T4 polynucleotide kinase (New England Biolabs)) end-labeled, 27-base oligonucleotide was added, and the DNAs were ethanol-precipitated. DNA was reconstituted in formamide-NaOH loading buffer and run in a 14% acrylamide denaturing gel and subsequently visualized using a PhosphorImager. For the experiments in Fig. 4, BSA or recombinant His$_6$-Est3p was titrated into the extension buffer at varying concentrations before addition of telomerase extract (5).

For Northern blot analysis, RNA was isolated from immunoprecipitation beads and detected by Northern blotting as described previously (15, 22). Whole cell RNA was prepared from 10 ml of mid-log phase cultures (26).

RESULTS

Est2p^{TEN} and Est3p Interact Directly in Vitro—The previously reported allele-specific suppression of temperature-sensitive mutations within the Est2p TEN domain by overproduction of Est3p (17) may reflect a direct interaction between the two proteins. To test this hypothesis, *EST3* was fused with an N-terminal His$_6$ tag, and the TEN domain of *EST2* (*EST2^{TEN}*; residues 1–162) was fused to the C terminus of MBP. Tagged proteins were individually expressed in *Escherichia coli* and purified to >95% apparent homogeneity (Fig. 1*A*). An ^{1}H-^{15}N heteronuclear single quantum correlation (HSQC) experiment was used to assess His$_6$-Est3p tertiary structure. Unfolding of the protein is expected to cause a collapse of cross-peaks in the region near 8 ppm. Instead, the HSQC of Est3p revealed excellent spectral dispersion with backbone amide peaks that range from ~6.1 to 9.9 ppm in the proton dimension (supplemental Fig. S1).

The individually purified proteins were mixed, and their co-purification was monitored. His$_6$-Est3p did not detectably associate with amylose resin alone (Fig. 1*D*, *lane 6*) or when co-in-

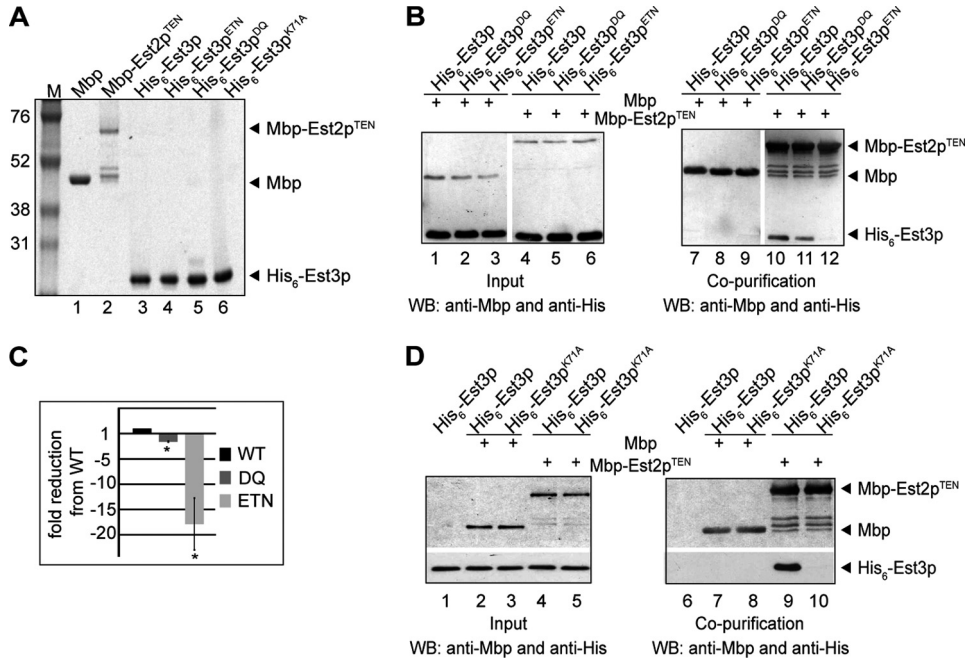

FIGURE 1. **MBP-Est2p^{TEN} interacts directly with His$_6$-Est3p.** *A*, Coomassie-stained gel of recombinant proteins purified from *E. coli*. Marker sizes (*M*) are shown in kDa. MBP, MBP-Est2p^{TEN}, and His$_6$-Est3p are 42, 62, and 21 kDa, respectively. The proteins were estimated to be >95% pure. *B*, 200 pmol of MBP or MBP-Est2p^{TEN} incubated as indicated (+) with 1 nmol of His$_6$-Est3p, His$_6$-Est3p^{DQ}, or His$_6$-Est3p^{ETN} and captured on amylose resin. Input (1% of total; *left panel*) and amylose-bound proteins (*right panel*) were analyzed by Western blotting (*WB*) using anti-MBP and anti-His antibodies. Data shown are representative of four independent experiments. *C*, quantification of data shown in *B*. -fold reduction in recovery of His$_6$-Est3p^{DQ} and His$_6$-Est3p^{ETN} compared with wild type was averaged over four independent experiments. *Bars* are S.E. Both His$_6$-Est3p^{DQ} and His$_6$-Est3p^{ETN} binding are statistically different from His$_6$-Est3p by one-tailed paired *t* test (*p* values 0.0002 and 0.0007, respectively) as denoted by *. *D*, 200 pmol of MBP or MBP-Est2p^{TEN} incubated as indicated (+) with 1 nmol of His$_6$-Est3p or His$_6$-Est3p^{K71A} and captured on amylose resin. Input (1% of total; *left panel*) and amylose-bound proteins (*right panel*) were analyzed by Western blotting using anti-MBP and anti-His antibodies. Data shown are representative of three independent experiments.

cubated with MBP (Fig. 1*B*, *lane 7*). In contrast, His$_6$-Est3p robustly co-purified with MBP-Est2p^{TEN} (Fig. 1*B*, *lane 10*), indicating that His$_6$-Est3p and MBP-Est2p^{TEN} bind directly *in vitro*.

To examine the specificity of the interaction between Est3p and Est2p^{TEN}, we created and characterized *EST3* mutants known or suspected to influence telomerase assembly and/or function. Based on structural modeling, these mutations are predicted to affect surface-exposed residues and to have minor effects on protein stability (27). Est3p^{K71A} (lysine 71 mutated to alanine) has been shown to disrupt telomere maintenance but retain assembly with telomerase *in vivo*, as assessed by co-purification of the mutant protein with TLC1 RNA (27). In contrast, individual mutations in residues glutamate 114, threonine 115, or asparagine 117 were shown to shorten telomeres and reduce Est3p association with TLC1 RNA (27). To disrupt this charged region completely, we simultaneously mutated all three residues to create Est3p$^{E114A,\ T115A,\ N117K}$ (Est3p^{ETN}). Aspartate 166 also contributes to the association of Est3p with TLC1 RNA (27). Because glutamine 167 is conserved in related fungal species, we mutated both residues to create Est3p$^{D166A,\ Q167A}$ (Est3p^{DQ}).

These mutant proteins were purified as His$_6$ fusion proteins from *E. coli* and their secondary structure characterized by circular dichroism. Both the wild-type Est3p and each of the altered Est3 proteins displayed strong evidence of secondary structure, suggesting that the amino acid changes did not strongly perturb protein folding (supplemental Fig. S2). Compared with the interaction observed for wild-type His$_6$-Est3p, co-purification of His$_6$-Est3p^{ETN} with MBP-Est2p^{TEN} was greatly decreased (Fig. 1, *B* and *C*; 17-fold, $p = 0.0007$). In contrast, the interaction between recombinant MBP-Est2p^{TEN} and His$_6$-Est3p^{DQ} was only slightly decreased compared with wild type (Fig. 1, *B* and *C*; 1.5-fold, $p = 0.0002$). The identification of point mutations that disrupt the Est3p/Est2p^{TEN} interaction *in vitro* suggests that the association between these two proteins is both direct and specific. Furthermore, residues near Glu^{114} contribute to the association of Est3p with the TEN domain of Est2p.

Surprisingly, no association between His$_6$-Est3^{K71A} and MBP-Est2p^{TEN} could be detected in the pulldown assay (Fig. 1*D*, *lane 10*), even though this mutant can assemble with the telomerase complex *in vivo* (27) (Fig. 2). This result may suggest that Est3p can assemble with telomerase through additional interactions *in vivo*. However, we cannot dismiss the possibility that mutation of lysine 71 to alanine disrupts the integrity of the recombinant protein.

EST3 Mutant Alleles Alter Telomerase Assembly and Function in Vivo—Because the *est3^{ETN}* and *est3^{DQ}* alleles evaluated in this study are different from those investigated previously (27), we characterized their *in vivo* phenotype. Telomerase assembly was monitored by co-immunoprecipitation of HA-tagged Est3p with TLC1 RNA and with Myc$_{18}$-tagged Est2p (Fig. 2). The strain background utilized lacked endogenous *EST3*. *EST2* was epitope-tagged at its N terminus by two-step integration of 18 copies of the Myc epitope at the endogenous locus. To avoid complications that might arise from measuring telomerase assembly in senescent strains, the epitope-tagged

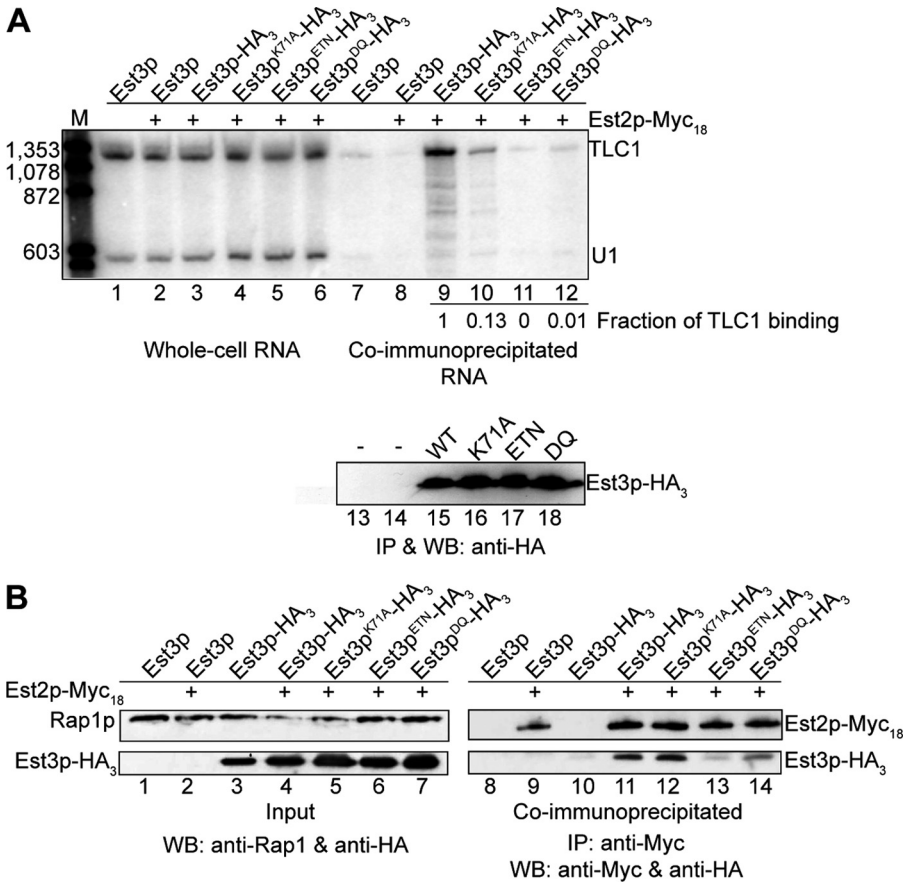

FIGURE 2. **Est3p^{ETN} shows reduced association with telomerase *in vivo*.** *A*, whole cell RNA (*lanes 1–6*) or anti-HA immunoprecipitations (*lanes 7–12*) were generated from yeast strains AVL78 (untagged; *lanes 1* and *7*) or YKF126 (*EST2-MYC$_{18}$ est3::KAN^R*) with pKF441 (*CEN EST3 URA3*) and pKF448^{HA} (*CEN EST3-HA$_3$ LEU2*), or pKF449^{HA} (2 μM *est3$^{K71A, ETN, or DQ}$-HA$_3$ LEU2*) as indicated. TLC1 and U1 RNA were detected by Northern blotting (*upper panel*); *M* is marker in bp. The amount of TLC1 retained in each co-immunoprecipitation (normalized to the wild-type value) is notated under *lanes 9–12*. This value was determined by first subtracting the amount of TLC1 bound nonspecifically (untagged Est3p; *lane 8*) from the amount of TLC1 observed in each lane and then dividing by the wild-type value (*lane 9*). Est3p-HA$_3$ recovery was measured by Western blotting (*WB*; *lower panel*; *lanes 13–18*) in the identical immunoprecipitation. Results are representative of two independent biological replicates (see supplemental Fig. S3). *B*, protein extracts were isolated from strains AVL78 (*lanes 1* and *8*), YKF126 containing plasmid pKF441 (*lanes 2* and *9*), YKF122 (*est3::KAN^R*) containing pKF442^{HA} (*CEN EST3-HA$_3$ URA3*; *lanes 3* and *10*), or YKF126 containing plasmids pKF441 and pKF448^{HA} or pKF449^{HA} mutants, as indicated. Anti-Myc immunoprecipitations were analyzed by Western blotting with monoclonal anti-Myc and anti-HA antibodies (*lanes 8–14*). Input (1% of total) was probed with anti-HA and anti-Rap1p antibodies as a loading control (*lanes 1–7*). Results are representative of two biologically independent experiments.

EST3 variants were expressed from a plasmid in the presence of an untagged *CEN EST3*-complementing plasmid. Previous work has shown that the untagged Est3 protein does not interfere appreciably with the ability of epitope-tagged Est3p to co-immunoprecipitate with its binding partners (27).

We first verified that TLC1 RNA levels are not affected by the *EST3* mutations. As shown in Fig. 2*A* (*lanes 1–6*), TLC1 RNA levels detected by Northern blotting from total cellular RNA are equivalent across strains. Est3p was immunoprecipitated from whole cell extract, and an aliquot was analyzed by Western blotting (Fig. 2*A*, *lower panel*). Each of the mutant proteins was expressed at a level equivalent to or slightly higher than wild-type Est3p (mutants are expressed from a high copy number 2 μm plasmid). TLC1 RNA was detected by Northern blotting in the identical immunoprecipitates (Fig. 2*A*, *lanes 7–12*). After correcting for minor nonspecific recovery of TLC1 RNA from control extract lacking the HA tag on Est3p (Fig. 2*A*, *lane 8*), the amount of TLC1 RNA immunoprecipitated with each mutant protein was expressed as a fraction of the association observed for wild-type Est3p. Highly congruent results were obtained in two independent biological replicates (Fig. 2*A* and supplemental Fig. S3). Est3p^{ETN}-HA$_3$ and Est3p^{DQ}-HA$_3$ showed very little if any residual association with TLC1, in agreement with the effects previously observed for the corresponding single amino acid mutations in *EST3*. Est3p^{K71A}-HA$_3$ consistently retained higher levels of association with TLC1 than the other mutants, but was reduced to ~10% of the wild-type level (Fig. 2*A*).

As an alternate measure of telomerase complex assembly, we monitored the co-immunoprecipitation of each Est3p variant with Myc$_{18}$-Est2p. In agreement with the effects on TLC1 association, Est3p^{ETN}-HA$_3$ and Est3p^{DQ}-HA$_3$ were reduced in their ability to co-immunoprecipitate with Myc$_{18}$-Est2p (Fig. 2*B*). Interestingly, Est3p^{K71A}-HA$_3$ immunoprecipitated with Myc$_{18}$-Est2p at a level similar to wild type. The discordance between the ability of Est3p^{K71A}-HA$_3$ to immunoprecipitate with TLC1 and Myc$_{18}$-Est2p suggests that the interaction between TLC1 RNA and Est3p (likely indirect) is more easily disrupted by the wash conditions than the interaction between Est2p and Est3p. In agreement with previous results (27), we

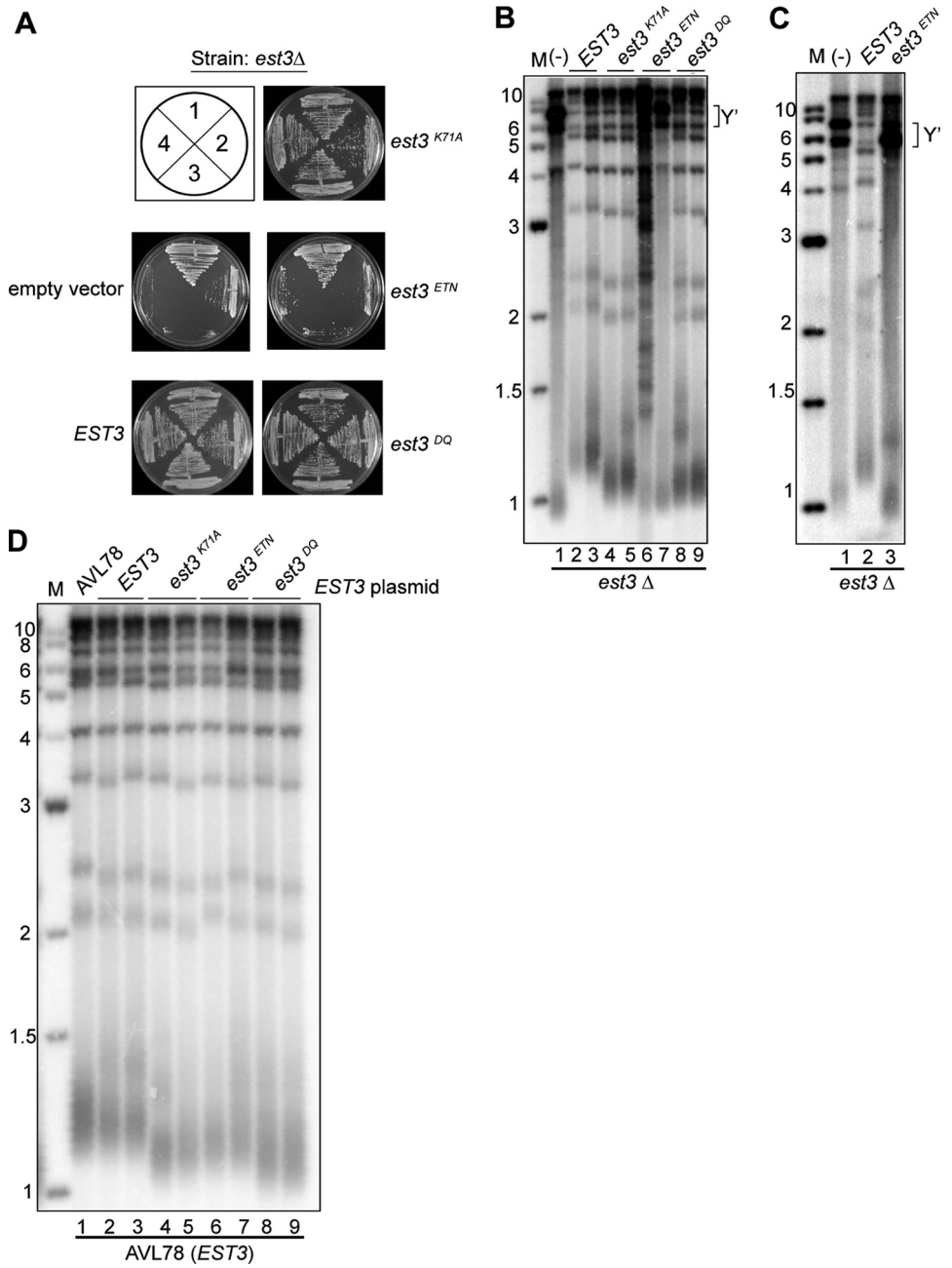

FIGURE 3. ***EST3^{ETN}* does not complement an *est3*Δ strain even when overexpressed.** *A*, yeast strain YKF122 complemented with pKF441 was transformed with pRS315 (*CEN LEU2* empty vector), pKF448 (*CEN EST3 LEU2*), or pKF448 mutants (*CEN est3$^{K71A, ETN,}$* or *^{DQ} LEU2*), and loss of the *URA3*-complementing plasmid was selected on plates containing 5-fluoroorotic acid. Cells were restreaked four times; *numbers* represent restreaks following loss of the complementing plasmid. *B*, DNA was extracted from cells grown in liquid culture from the third restreak of strains shown in *A*. DNA was digested with XhoI, Southern blotted, and probed with a telomeric fragment. (−) indicates the empty vector control. Y′ elements are *bracketed*. Two independent transformants are shown. *M* is marker in kb. *C*, YKF122 (*est3::KAN^{R}*) complemented with pKF441 (*CEN EST3 URA3*) was transformed with pRS425 alone (2 μM *LEU2*), *lane 1*; pKF449 (2 μM *EST3 LEU2*), *lane 2;* or pKF449^{ETN} (2 μM *EST3^{ETN} LEU2*), *lane 3*. After selection for loss of the complementing plasmid on plates containing 5-fluoroorotic acid, cells were restreaked three times on plates lacking leucine. Telomere blots were performed as described in *B*. Y′ elements are *bracketed*. *D*, AVL78 was transformed with pKF449 (2 μM *EST3 LEU2*) expressing the indicated *EST3* alleles. After three successive restreaks, genomic DNA was digested with XhoI, blotted, and probed with a telomeric fragment. Two biological replicates are shown. The parental wild-type strain (AVL78) is shown for reference.

conclude that the residues near glutamate 114 and aspartate 166 are important for Est3p assembly with telomerase, whereas residue lysine 71 plays a less critical role *in vivo*.

est3^{ETN} Does Not Retain Function in Vivo—To address the ability of the EST3 variants to support telomere replication, each allele was expressed from a low copy number centromere plasmid in yeast lacking endogenous *EST3*. The resulting strains were monitored for the ability to support growth over three consecutive restreaks on solid medium. As expected, the yeast expressing wild-type *EST3* maintained robust cellular growth, whereas the empty vector control senesced after three restreaks (Fig. 3*A*). Interestingly, the strain expressing *est3^{ETN}* resembled the empty vector control for growth (Fig. 3*A*), whereas *est3^{K71A}* and *est3^{DQ}* looked similar to wild type. As a more sensitive measure of telomerase function, the telomere length of cells taken from the final restreak was measured by

Southern blotting. In cells with normal telomerase function, XhoI releases a terminal fragment of ~1.2–1.3 kb from chromosomes possessing one or more subtelomeric Y′ elements (Fig. 3*B*, *lanes 2* and 3). In contrast, cells containing either empty vector or expressing *est3*^{ETN} displayed hallmarks of telomerase dysfunction (Fig. 3*B*, *lanes 1*, *6*, and *7*). Cells that are unable to utilize telomerase instead use a *RAD52*-dependent recombination pathway to maintain telomeres, manifested on the Southern blot as stochastic lengthening of the TG-rich telomeric repeats (Fig. 3*B*, *lane 6*) or amplification of Y′ elements (*brackets*, Fig. 3*B*, *lanes 1* and *7*) (28). Expression of *est3*^{ETN} from a high copy number 2-μm plasmid allowed the protein to accumulate at wild-type levels (Fig. 2*B*, compare *lanes 4* and *6*) but did not improve complementation for either growth (data not shown) or telomere length (Fig. 3*C*), indicating that low protein levels alone do not account for the lack of telomere maintenance.

Although both *est3*^{DQ} and *est3*^{K71A} supported normal cellular growth (Fig. 3*A*), the telomeres in cells expressing these *EST3* alleles were maintained at a length shorter than wild type (Fig. 3*B*), similar to a previous report (27). All of the *est3* alleles were dominant negative when overexpressed in the presence of wild-type Est3p, suggesting that they are expressed and retain some function (Fig. 3*D*). Together, these data reveal that residues Glu^{114}, Thr^{115}, and Asn^{117} are critically important for telomerase assembly both *in vivo* and *in vitro*, whereas Asp^{166} and Gln^{167} appear to have a lesser role *in vitro*. As described previously (27), Lys^{71} has a less severe effect on telomerase assembly *in vivo*, although mutation of this residue to alanine disrupts the interaction between Est3p and the TEN domain of Est2p *in vitro* (see "Discussion").

Est3p Stimulates Telomerase Activity in Vitro—The function of Est3p in *S. cerevisiae* has remained elusive since its discovery as a telomerase complex component (6). Although early studies did not detect an obvious loss of catalytic activity upon *EST3* deletion (20), more recent studies of *S. castelli* and *C. albicans* have demonstrated roles for these Est3p homologs during primer extension *in vitro* (18, 21). These observations raise the possibility that Est3p from *S. cerevisiae* may have a similar function but that the particular assay conditions utilized either minimize or mask that effect.

To address this issue, we measured the ability of recombinant Est3p to stimulate the primer extension activity of partially purified yeast telomerase. Biotin-labeled yeast telomeric primers were bound to streptavidin beads and incubated in the presence of radiolabeled nucleotides and wild-type telomerase extract that was partially purified over DEAE and Mono Q resins (5, 29). As previously demonstrated, yeast telomerase adds seven nucleotides (5′-GGTGTGG) to the end of the primer and then terminates elongation. Titration of His$_6$-Est3p into this reaction increased overall telomerase activity in a dose-dependent manner, whereas a BSA control did not (Fig. 4*A*). Importantly, Est3p does not appear to affect the processivity of telomerase in this assay because neither the maximal length of the extended product nor the relative intensity of each band is altered. We conclude that Est3p (like Est1p) (5) stimulates telomerase activity by increasing the fraction of extended primers.

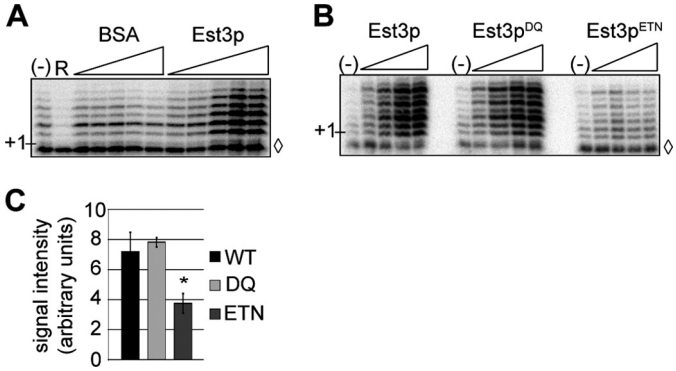

FIGURE 4. **Recombinant Est3p stimulates telomerase activity *in vitro* in a manner dependent on the Est3p/Est2p^{TEN} interaction.** *A*, partially purified telomerase extracts were prepared from YPH499 cells and incubated with a 7-base 3′-overhang-immobilized DNA primer in the presence of dTTP and [α-^{32}P]dGTP. In *lane R*, RNaseA was added to telomerase prior to addition of the primer. BSA or recombinant His$_6$-Est3p (0.5, 1, 2.5, 5, or 10 μM) was titrated into DNA extension reactions as indicated. (−) indicates basal telomerase activity. ◊ indicates a 27-mer loading control added prior to DNA precipitation. *B*, recombinant His$_6$-Est3p (wild type or indicated mutant; 0.25, 0.5, 1, 2.5, and 5 μM) was titrated into DNA extension reactions as described above. (−) indicates basal telomerase activity. ◊ indicates a 27-mer loading control added prior to DNA precipitation. *C*, recombinant His$_6$-Est3p (wild type or mutant) was added at 2.5 μM to DNA extension reactions. Signal intensity of three replicates was determined using ImageQuant software, and significance was assessed using an analysis of variance (ANOVA) post hoc Dunnett's (control = His$_6$-Est3p). The stimulatory activity of His$_6$-Est3p^{ETN} was lower than wild-type His$_6$-Est3p ($p = 0.03$), whereas His$_6$-Est3p^{DQ} activity was similar to wild type ($p = 0.87$). *Bars* represent S.E., and * denotes a p value <0.05.

Having established that recombinant Est3p stimulates primer extension by telomerase, we next determined the effect of each previously characterized mutant Est3 protein in this assay. Est3p^{ETN} was significantly reduced in its ability to stimulate telomerase activity compared with wild-type Est3p (Fig. 4, *B* and *C*; $p = 0.03$). Because the association of Est3p^{ETN} with the Est2p TEN domain was dramatically reduced *in vitro* (Fig. 1), this result suggests that the interaction between Est3p and Est2p^{TEN} is required for telomerase stimulation. Consistent with its ability to bind Est2p^{TEN} *in vitro*, Est3p^{DQ} retained the capacity to stimulate telomerase (Fig. 4, *B* and *C*; $p = 0.87$). Given the reduced assembly and activity of this mutant *in vivo*, this result suggests that Est3p^{DQ} affects a different, yet uncharacterized function of Est3p. Overall, these data show that *S. cerevisiae* Est3p can stimulate telomerase activity in a manner dependent on direct interaction with Est2p^{TEN}.

DISCUSSION

Although the major components of yeast telomerase have been known for more than a decade, it has been difficult to determine the details of subunit interactions within the complex. Here we provide the first evidence of a direct Est2p/Est3p interaction in *S. cerevisiae*. Recombinant Est3p binds the purified TEN domain of Est2p *in vitro*, and this interaction is largely dependent upon several predicted surface residues of Est3p, including residues glutamate 114, threonine 115, and asparagine 117 (Fig. 1). Additionally, recombinant Est3p stimulates telomerase activity *in vitro* in a manner dependent upon the Est2p TEN domain interaction (Fig. 4). This result reconciles the effect of *S. cerevisiae* Est3p with previous experiments showing that Est3p homologs in related yeast species influence the enzymatic activity of telomerase (18, 21).

A Direct Est2p/Est3p Interaction Contributes to the Assembly of Est3p with Telomerase—We showed previously that Est1p stimulates the assembly of Est3p with telomerase (15). However, our failure to detect an Est1p/Est3p interaction by co-immunoprecipitation from cell extract in the absence of Est2p suggested that Est1p might not be the primary binding site for Est3p (15). Additionally, *EST1* function is bypassed in a strain expressing a Cdc13-Est2 fusion protein, whereas *EST3* remains essential (4). This result implies that Est3p can, in some circumstances, assemble and contribute to telomerase function in the absence of Est1p. Prior to work presented here, genetic results revealed that overexpression of Est3p suppresses mutations located in the Est2p TEN domain, but evidence for a direct interaction between these components was lacking (17).

Here we have combined an *in vitro* co-purification assay using recombinant proteins with experiments that assess both RNA and protein interactions in the native telomerase complex to gain a clearer understanding of telomerase complex assembly. Using these assays, we demonstrate that the Est2p TEN domain (residues 1–162) interacts directly with Est3p *in vitro* (Fig. 1). Mutation of three predicted surface-exposed residues (Glu^{114}, Thr^{115}, and Asn^{117}) of Est3p (27) significantly perturbs this interaction *in vitro*, while also disrupting the assembly of Est3p with telomerase *in vivo* (Figs. 1 and 2).

Interestingly, the $est3^{DQ}$ mutation decreases the co-immunoprecipitation of Est3p with both TLC1 RNA and Myc_{18}-Est2p *in vivo* (Fig. 2), but has a fairly minor (< 2-fold) effect on Est2p TEN binding *in vitro* (Fig. 1, *B* and *C*). One interpretation of these data is that the interaction between Est3p and $Est2p^{TEN}$ is insufficient for the assembly of Est3p with the telomerase complex *in vivo*, consistent with a model in which Est3p makes multiple contacts with telomerase components. This proposal is consistent with the recent report that Est3p interacts directly with Est1p (16).

However, because telomere length is only moderately affected by the DQ mutation, it is also possible that the co-immunoprecipitation experiment overemphasizes the defect of Est3p association *in vivo*. Indeed, even though the general trends are the same for $Est3p^{ETN}$-HA_3 and $Est3p^{DQ}$-HA_3, each mutation has an apparently more severe effect on TLC1 RNA association than on the ability to co-immunoprecipitate with Myc_{18}-Est2p (compare Fig. 2*A*, *lanes 11* and *12*, with Fig. 2*B*, *lanes 13* and *14*), suggesting that TLC1 RNA might be more sensitive to co-immunoprecipitation conditions than Est2p. This effect is even more pronounced with the $Est3p^{K71A}$-HA_3 mutation. Although the co-immunoprecipitation of TLC1 is reduced to ~10% of wild-type levels, the association of $Est3p^{K71A}$-HA_3 with Myc_{18}-Est2p is equivalent to that of wild-type Est3p. This difference may arise because Est3p and Est2p interact directly, whereas Est3p and TLC1 do not.

Although $Est3p^{K71A}$-HA_3 and Myc_{18}-Est2p co-immunoprecipitate from cellular extract, the $est3^{K71A}$ mutation abolishes the *in vitro* interaction between MBP-$Est2p^{TEN}$ and His_6-Est3p (Fig. 1*D*). This result may suggest that a second site of interaction between Est3p and telomerase, such as the interaction with Est1p (16), can mediate Est3p assembly when the TEN domain interaction is compromised. If true, the $est3^{ETN}$ mutation must disrupt both contacts. However, we cannot eliminate the possibility that the $Est3^{K71A}$ protein has defects *in vitro* (such as a minor disruption in tertiary structure) that are not reflected *in vivo*.

S. cerevisiae Est3p Contributes to Telomerase Activity in Vitro—Two recent papers have demonstrated that the Est3p homologs in *C. albicans* and *S. castelli* influence telomerase activity *in vitro* (18, 21). We report here that *S. cerevisiae* Est3p also stimulates basal telomerase activity (Fig. 4). Interestingly, His_6-$Est3p^{DQ}$, the mutant that retains assembly with the Est2p TEN domain, stimulates telomerase activity, whereas two mutants that compromise the Est3p/$Est2p^{TEN}$ interaction ($est3^{ETN}$ and $est3^{K71A}$) do not (Fig. 4 and data not shown). These results suggest that Est3p requires interaction with the Est2p TEN domain to mediate its stimulatory effect. The requirement for this interaction in the stimulation assay may simply reflect a defect in the recruitment of recombinant Est3p to the telomerase complex *in vitro*. However, it is also plausible that the stimulatory effect of Est3p requires a specific interaction with the TEN domain that is separable from complex assembly.

Are Est3 and TPP1 Evolutionarily Related?—TPP1 is a member of the telomere-binding shelterin complex in mammals and influences the processivity of telomerase *in vitro* (30, 31). Based on prediction algorithms, fungal Est3p has a similar structure to the oligonucleotide/oligosaccharide-binding (OB) fold domain of TPP1, although this observation alone does not imply an evolutionary relationship between the two proteins (27, 32). Intriguingly, deletion of the TPP1 OB fold disrupts telomerase localization to the telomere in human cells (33). Additionally, a sequence-specific interaction between TPP1 and the human TEN domain of TERT is important for telomerase processivity (34). Our observation that the Est2p TEN domain mediates a critical interaction with Est3p that influences both telomerase assembly *in vivo* and stimulation of telomerase activity *in vitro* provides an intriguing parallel between the two proteins. The glutamate 114, threonine 115, and asparagine 117 of the Est3p primary structure align near some surface-exposed residues within a small α-helix of the OB fold of TPP1: arginine 159, glutamate 160, aspartate 163, and threonine 164. Determining whether these residues influence telomerase function in higher eukaryotes could give insight into a possible evolutionary relationship between Est3p and TPP1.

Acknowledgments—We thank Drs. Victoria Lundblad, Virginia Zakian, and Laura Mizoue for strains and reagents; L. M. and Dr. Markus Voehler for assistance with NMR and CD; L. M. and the Center for Structural Biology at Vanderbilt University for help with protein purification; Dr. David Friedman for mass spectrometry analysis; Margaret Platts for technical assistance; and Jenifer Ferguson and Dr. Christopher Brown for critical reading of the manuscript.

Note Added in Proof—A direct interaction between Est3p and the TEN domain of the Est2p homologs in two *Candida* species was recently reported by Yan *et al.* (Yan, W.-F., Chico, L., Lei, M., and Lue, N. F. (2011) *Proc. Natl. Acad. Sci. U.S.A.* doi: 10.1073/pnas.1017855108).

REFERENCES

1. Osterhage, J. L., and Friedman, K. L. (2009) *J. Biol. Chem.* **284,** 16061–16065

2. Lingner, J., Hughes, T. R., Shevchenko, A., Mann, M., Lundblad, V., and Cech, T. R. (1997) *Science* **276,** 561–567
3. Singer, M. S., and Gottschling, D. E. (1994) *Science* **266,** 404–409
4. Evans, S. K., and Lundblad, V. (1999) *Science* **286,** 117–120
5. DeZwaan, D. C., and Freeman, B. C. (2009) *Proc. Natl. Acad. Sci. U.S.A.* **106,** 17337–17342
6. Hughes, T. R., Evans, S. K., Weilbaecher, R. G., and Lundblad, V. (2000) *Curr. Biol.* **10,** 809–812
7. Lendvay, T. S., Morris, D. K., Sah, J., Balasubramanian, B., and Lundblad, V. (1996) *Genetics* **144,** 1399–1412
8. Lundblad, V., and Szostak, J. W. (1989) *Cell* **57,** 633–643
9. Livengood, A. J., Zaug, A. J., and Cech, T. R. (2002) *Mol. Cell. Biol.* **22,** 2366–2374
10. Seto, A. G., Livengood, A. J., Tzfati, Y., Blackburn, E. H., and Cech, T. R. (2002) *Genes Dev.* **16,** 2800–2812
11. Chappell, A. S., and Lundblad, V. (2004) *Mol. Cell. Biol.* **24,** 7720–7736
12. Seto, A. G., Zaug, A. J., Sobel, S. G., Wolin, S. L., and Cech, T. R. (1999) *Nature* **401,** 177–180
13. Fisher, T. S., Taggart, A. K., and Zakian, V. A. (2004) *Nat. Struct. Mol. Biol.* **11,** 1198–1205
14. Bianchi, A., Negrini, S., and Shore, D. (2004) *Mol. Cell* **16,** 139–146
15. Osterhage, J. L., Talley, J. M., and Friedman, K. L. (2006) *Nat. Struct. Mol. Biol.* **13,** 720–728
16. Tuzon, C. T., Wu, Y., Chan, A., and Zakian, V. A. (2011) *PLoS Genet.* **7,** e1002060
17. Friedman, K. L., Heit, J. J., Long, D. M., and Cech, T. R. (2003) *Mol. Biol. Cell* **14,** 1–13
18. Lee, J., Mandell, E. K., Rao, T., Wuttke, D. S., and Lundblad, V. (2010) *Nucleic Acids Res.* **38,** 2279–2290
19. Sharanov, Y. S., Zvereva, M. I., and Dontsova, O. A. (2006) *FEBS Lett.* **580,** 4683–4690
20. Lingner, J., Cech, T. R., Hughes, T. R., and Lundblad, V. (1997) *Proc. Natl. Acad. Sci. U.S.A.* **94,** 11190–11195
21. Hsu, M., Yu, E. Y., Singh, S. M., and Lue, N. F. (2007) *Eukaryot. Cell* **6,** 1330–1338
22. Friedman, K. L., and Cech, T. R. (1999) *Genes Dev.* **13,** 2863–2874
23. Sikorski, R. S., and Hieter, P. (1989) *Genetics* **122,** 19–27
24. Christianson, T. W., Sikorski, R. S., Dante, M., Shero, J. H., and Hieter, P. (1992) *Gene* **110,** 119–122
25. Toogun, O. A., Zeiger, W., and Freeman, B. C. (2007) *Proc. Natl. Acad. Sci. U.S.A.* **104,** 5765–5770
26. Chapon, C., Cech, T. R., and Zaug, A. J. (1997) *RNA* **3,** 1337–1351
27. Lee, J., Mandell, E. K., Tucey, T. M., Morris, D. K., and Lundblad, V. (2008) *Nat. Struct. Mol. Biol.* **15,** 990–997
28. Chan, C. S., and Tye, B. K. (1983) *Cell* **33,** 563–573
29. Toogun, O. A., Dezwaan, D. C., and Freeman, B. C. (2008) *Mol. Cell. Biol.* **28,** 457–467
30. de Lange, T. (2005) *Genes Dev.* **19,** 2100–2110
31. Wang, F., Podell, E. R., Zaug, A. J., Yang, Y., Baciu, P., Cech, T. R., and Lei, M. (2007) *Nature* **445,** 506–510
32. Yu, E. Y., Wang, F., Lei, M., and Lue, N. F. (2008) *Nat. Struct. Mol. Biol.* **15,** 985–989
33. Abreu, E., Aritonovska, E., Reichenbach, P., Cristofari, G., Culp, B., Terns, R. M., Lingner, J., and Terns, M. P. (2010) *Mol. Cell. Biol.* **30,** 2971–2982
34. Zaug, A. J., Podell, E. R., Nandakumar, J., and Cech, T. R. (2010) *Genes Dev.* **24,** 613–622